

Thin-film β - MoO_3 Supported on α - Fe_2O_3 as Shell-Core Catalyst for the Selective Oxidation of Methanol to Formaldehyde

Guojun Shi, Thomas Franzke, Miguel D. Sánchez, Wei Xia, Frederik Weis, Martin Seipenbusch, Gerhard Kasper, Martin Muhler*

The ultimate goal of catalysis research is to control the activity and selectivity of catalysts by tuning their structural and electronic properties. A key requirement to achieve this goal is the well-controlled synthesis of catalysts, which is a sophisticated art due to their complexity and evolution under reaction conditions.^[1] Nanotechnology offers a significant potential in designing and building catalysts at an/a atomic or molecular level,^[2] and catalysis research is considered to be strongly linked to nanoscience.^[3,4] It was suggested that catalysts should be regarded as inorganic polymers rather than as close-packed crystals, which can be synthesized by assembling molecular building blocks and linkers.^[3,4] Molybdenum oxide films have a high potential in chromogenic,^[5] sensing^[6] and catalytic applications.^[7] For instance, a change in the color of molybdenum oxides can be induced electrically, thermally and by light, and also reversibly by the intercalation of cations such as Li^+ and H^+ .^[5,8] Semiconducting molybdenum oxide films are used in gas-sensing devices, because the electrical conductivity changes as a function of coverage allowing to detect CO and NO concentration as low as 10 ppm in air.^[9] Molybdenum oxide films are also used for the selective oxidation of lower olefins.^[10-12]

Formaldehyde is one of the most important bulk chemicals produced over molybdenum oxide-based catalysts by selective oxidation of methanol. Routray et al.^[13] found that the supported $\text{MoO}_3/\text{Fe}_2\text{O}_3$ catalysts possessed catalytic activity comparable to that of the conventionally used bulk iron molybdate catalysts with excess MoO_3 . They attributed the enhanced activity of bulk iron molybdate catalysts with excess MoO_3 to the formation of a MoO_x monolayer on the surface, which exposes the catalytically active sites that are continuously replenished by this excess crystalline MoO_3 phase. Street and Goodman^[14] investigated the nature of MoO_3 and $\text{MoO}_3/\text{Al}_2\text{O}_3$ ultra-thin films and their interactions with methanol. They identified the vibrational features associated with

terminal $\text{Mo}=\text{O}$ and bridging $\text{Mo}-\text{O}-\text{Mo}$ species in tetrahedral molybdate and found a decrease in the $\text{Mo}=\text{O}$ intensity of unsupported molybdate after several runs of methanol adsorption/desorption and a recovery of the $\text{Mo}=\text{O}$ intensity after subsequent annealing. An earlier study suggested that methanol oxidation over MoO_3 catalysts involves methoxy intermediates chemisorbed on oxygen vacancy sites.^[15] Formaldehyde and CO are assumed to be mainly produced from methoxy species on terminal oxygen ($\text{Mo}=\text{O}$) vacancy sites, while bridged oxygen ($\text{Mo}-\text{O}-\text{Mo}$) vacancy sites are considered responsible for the production of dimethyl ether, dimethoxymethane and methyl formate.^[15]


Machiels and Sleight^[16] investigated methanol oxidation to formaldehyde over MoO_3 -based catalysts and found that pure MoO_3 acts very similar to ferric molybdate with respect to selectivities, activation energies, and reaction orders except a significantly lower activity. They obtained evidence using deuterated methanol that the rate-determining step of the reaction is the abstraction of hydrogen from the methyl group of adsorbed methoxy on the MoO_3 -based catalysts. Sleight and coworkers^[17] confirmed these results quantitatively by studying the adsorption of methanol on MoO_3 , the subsequent decomposition of methoxy yielding formaldehyde and H_2O , and the uptake of oxygen individually by means of TPD/microgravity.

Several techniques have been developed to synthesize MoO_3 films, such as vacuum evaporation of MoO_3 ,^[18] hot filament metal oxide deposition,^[9] sputtering deposition,^[10] plasma assisted molecular beam epitaxy,^[20] and chemical vapor deposition (CVD).^[21] Molybdenum trioxide crystallizes as thermodynamically stable α - MoO_3 (orthorhombic) and as two metastable phases: β - MoO_3 (monoclinic) and h - MoO_3 (hexagonal). α - MoO_3 is constituted of $[\text{MoO}_6]$ octahedra sharing edges and corners, forming zigzag chains and unique layers parallel to the (010) plane. Monoclinic β - MoO_3 possesses a ReO_3 -related structure, where the $[\text{MoO}_6]$ octahedra share corners to form a distorted cube. h - MoO_3 is constructed of the zigzag chains of $[\text{MoO}_6]$ octahedra as the building blocks but interlinked through the *cis*-position, presenting a hexagonal crystalline structure with large one-dimensional tunnels.^[8] It was reported that monoclinic β - MoO_3 was catalytically more active than orthorhombic α - MoO_3 in the selective oxidation of methanol to formaldehyde.^[22] In the present work, β - MoO_3 thin-film catalysts were synthesized for the first time by one-step CVD of $\text{Mo}(\text{CO})_6$ on α - Fe_2O_3 applying a vertical hot-wall reactor. The crystalline phase, morphology, texture and surface properties of the resulting MoO_3 films with thicknesses of 2–8 nm were characterized in depth, and the selective oxidation of methanol to formaldehyde was used as catalytic probe reaction.

The specific surface areas and the molybdenum loadings of the CVD samples are summarized in **Table 1**. Under the experimental conditions applied, more than 80% of the molybdenum precursor was deposited on the α - Fe_2O_3 particles used as substrate in spite of

[*] Dr. G. Shi, Dr. T. Franzke, Dr. M. D. Sánchez, Dr. W. Xia, Prof. Dr. M. Muhler
Laboratory of Industrial Chemistry
Ruhr-University Bochum
Universitätsstraße 150 44801 Bochum
Fax: (+49) 234 32-14115
E-mail: muhler@techem.ruhr-uni-bochum.de
Homepage: <http://www.techem.rub.de>

F. Weis, Dr. M. Seipenbusch, Prof. Dr. G. Kasper
Institute for Mechanical Process Engineering and Mechanics
Karlsruhe Institute of Technology
Straße am Forum 8, 76131 Karlsruhe

 The authors gratefully acknowledge financial support by the German Research Foundation (DFG, MU 1327/5-1) and thank Michael Becker for experimental support.

the rather high Mo loading. There were only small changes in the specific surface areas due to the coating with MoO₃, and the SEM images (Figure S1) obtained after coating did not reveal any significant changes of the morphology. This is in agreement with the BET surface areas of the synthesized catalysts (Table 1) indicating that the coated MoO₃ species are well dispersed on the surface of the substrate.

Table 1. Physical properties of samples with different Mo loadings calcined at 673 K.

Sample	S _{BET} (m ² /g)	Nominal loading		Actual loading	
		Mo (wt.%)	Mo:Fe (atomic)	Mo (wt.%)	Mo:Fe (atomic)
Fe ₂ O ₃	6.2	-	-	-	-
MoFe5-673	7.4	5.5	0.05	4.7	0.042
MoFe10-673	6.4	10.2	0.10	9.1	0.088
MoFe20-673	6.0	17.6	0.20	15.8	0.172

The TEM images shown in Figure 1 exhibit direct evidence that MoO₃ was homogeneously deposited on the surface of the substrate. The irregular shape of the Fe₂O₃ particles is shown in Figure 1A. A layer of about 2.5 nm was formed for the sample MoFe5-673 on the substrate (Figure 1B). The sample MoFe10-673 and the sample MoFe20-673 display uniform layers with a thickness of about 5 and 8 nm, respectively. These results indicate clearly that homogeneous MoO₃ films were generated on the surface of the substrate by the CVD of Mo(CO)₆ in the presence of O₂, and that higher Mo loadings result in thicker layers. For a simple estimate the density of bulk MoO₃ (4.96 g/cm³), the specific surface area of the substrate α-Fe₂O₃, and the actual Mo loadings were used. It was found (Figure S2) that the film thickness observed by TEM was just a little higher than that obtained by the calculation.

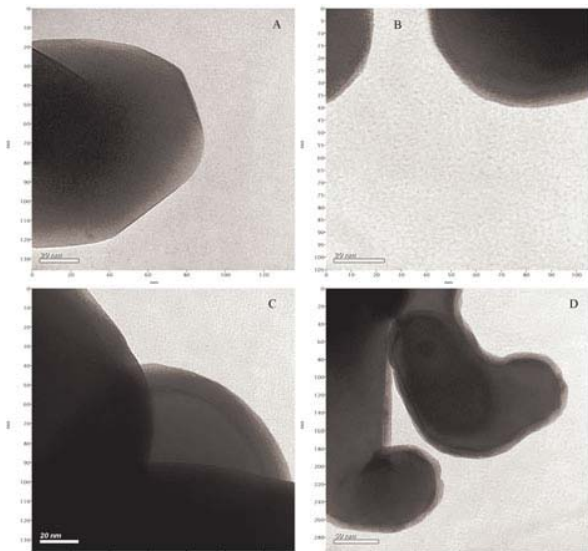


Figure 1. TEM images of (A) Fe₂O₃, (B) MoFe5-673, (C) MoFe10-673 and (D) MoFe20-673.

Figure 2A shows the XRD patterns of the substrate Fe₂O₃ and the samples synthesized at 673 K with different Mo loadings. Only Fe₂O₃ diffraction peaks were observed for sample MoFe5-673, which is attributed to the low Mo loading and the resulting low thickness of the MoO₃ film. The weak (100) diffraction peak of β-MoO₃ was detected for MoFe10-673 in agreement with the TEM-derived MoO₃ film thickness of about 5 nm. For the MoFe20-673

sample, stronger (100), (200) and (111) XRD diffraction peaks were observed.

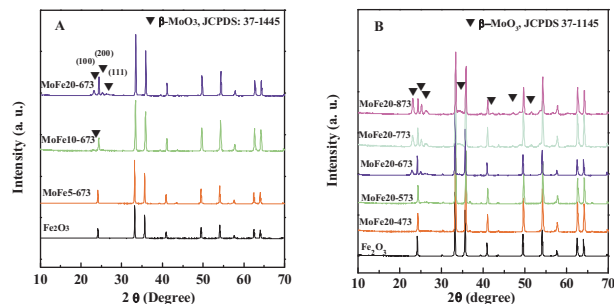


Figure 2. XRD patterns of samples synthesized with different (A) Mo loadings and (B) calcination temperatures.

As a metastable MoO₃ phase, the monoclinic β-MoO₃ phase can be transformed to the orthorhombic α-phase.^[24] McCarron III^[22] synthesized β-MoO₃ powder by drying molybdic acid and found that the resulting β-MoO₃ was transformed to α-MoO₃ when heating it higher than 720 K. It is interesting to note that the β-MoO₃ phase in the synthesized MoO₃/Fe₂O₃ samples was retained even after calcination in air at 873 K (Figure 2B). Obviously, the strong interaction between the Fe₂O₃ support and the β-MoO₃ film prevents its transformation into the thermodynamically favored α-MoO₃ phase.

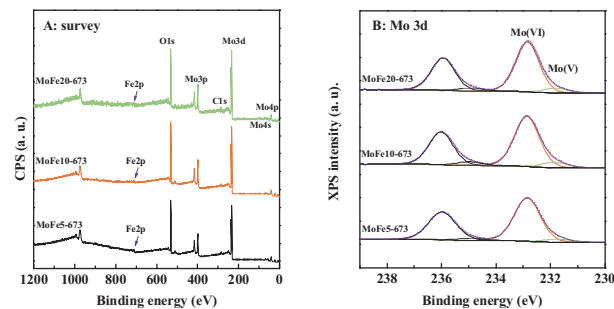


Figure 3. (A) Survey and (B) Mo 3d XP spectra of MoO₃/Fe₂O₃ samples with increasing MoO₃ loading.

The TEM images clearly show that the synthesized MoO₃/Fe₂O₃ samples have a shell-core structure, in which the Fe₂O₃ core is homogeneously covered by a thin β-MoO₃ film. XPS as a surface-sensitive technique probes the surface element distribution and surface chemical state of the investigated samples averaging within an area of about 0.5 mm² under the applied conditions. The XP spectra of the survey scan and the Mo 3d region are shown in Figure 3. Strong Mo signals were observed for all MoO₃/Fe₂O₃ samples, and, correspondingly, the Fe 2p XPS peaks were very weak. According to the elemental analysis based on ICP-OES, the bulk Mo/Fe atomic ratios of MoFe5-673, MoFe10-673 and MoFe20-673 are 0.042, 0.088 and 0.172, respectively (Table 1). The Mo/Fe surface atomic ratio derived from XPS are 9.6, 19.5 and 19.5, respectively (Table S1). The detected traces of Fe species may be due to small defects in the MoO₃ film, or damages of the shell-core structure during grinding. Thus, the synthesized samples were confirmed by XPS to have an essentially perfect shell-core structure.

The Mo 3d XP peaks mainly originate from Mo(VI) (Figure 3B) with Mo 3d_{5/2} binding energies of about 232.8 eV irrespective of the Mo concentration (Table S1) in line with the XRD results for the MoFe10-673 and MoFe20-673 catalysts. In case of the MoFe5-673

catalyst, the XPS results show that also its surface is mainly composed of Mo(VI) species, which are below the XRD detection limit. Less than 10% of Mo(V) species were detected on the samples studied (Figure 3B, Table S1) in agreement with the results reported by Al-Shihry et al.^[25] The presence of Mo(V) points to an influence of the α -Fe₂O₃ core enhancing the reducibility of Mo(VI). In addition, the Mo 3d peak width (FWHM) shows a decrease with increasing film thickness of MoO₃ (Table S1). The width was attributed to charge-induced broadening of non-conducting samples associated with the photoemission process.^[19]

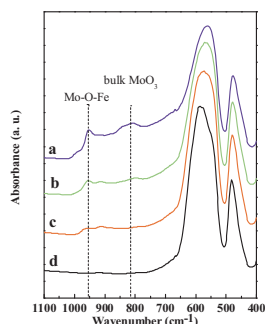


Figure 4. FTIR spectra of (a) MoFe20-673, (b) MoFe10-673, (c) MoFe5-673, and (d) Fe₂O₃.

Figure 4A shows the FTIR spectra of the catalysts. It is clearly seen that there are two groups of bands at 810-820 cm⁻¹ and around 960 cm⁻¹ on the synthesized β -MoO₃/Fe₂O₃ samples. The former can be assigned to the bulk MoO₃ phase, which is in line with the XRD patterns shown in Figure 2A, and the latter can be attributed to linking Mo-O-Fe species.^[26,27] In addition to the presence of a β -MoO₃ shell confirmed by XRD (Figure 2), the IR results indicate that there are Mo-O-Fe links formed at the interface due to strong interactions between β -MoO₃ and α -Fe₂O₃. Additionally, it is also interesting to note that the amount of surface acidic sites increased when decreasing the Mo loading (**Figure S3**), which can be attributed to the influence of the Mo-O-Fe links when the β -MoO₃ film is close to a monolayer (**Table S2**)^[28].

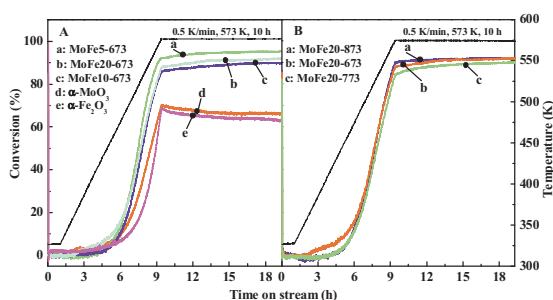


Figure 5. Methanol conversion over the catalysts synthesized with different (A) Mo loadings and (B) calcination temperatures.

Figure 5 shows the methanol conversion over the synthesized catalysts. It was found that using the α -Fe₂O₃ support results in a methanol conversion of around 65% at 573 K, and that bulk α -MoO₃ as a reference catalyst reaches a methanol conversion of about 68% at the same temperature (Figure 5A). The synthesized β -MoO₃/Fe₂O₃ catalysts displayed a much higher low-temperature activity from 323 K to 573 K. During 10 h of time on stream at 573 K, all β -MoO₃/Fe₂O₃ catalysts exhibited a 20% higher degree of methanol conversion than α -Fe₂O₃ and α -MoO₃ with the catalyst MoFe5-673 with the lowest Mo loading achieving slightly higher degrees of conversion than the other two β -MoO₃/Fe₂O₃ catalysts

with higher Mo loading. Additional experimental results showed that the methanol conversion increased to 98% at 573 K when decreasing the Mo loading to 0.5% (**Figure S4**). There was no obvious difference in conversion observed for the catalysts calcined at different temperatures (Figure 5B & Figure S4), and it is interesting to note that MoFe20-873-24h, which was calcined in flowing air for 24 h, exhibited a higher methanol conversion (Figure S4).

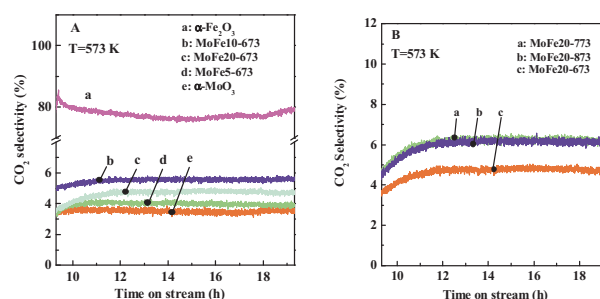


Figure 6. CO₂ selectivities of the catalysts synthesized with different (A) Mo loadings and (B) calcination temperatures.

In the methanol oxidation reaction, some possible byproducts include CO, CO₂, dimethyl ether, methyl formate, and dimethoxymethane (DMM).^[23] **Figure 6** shows the CO₂ selectivities achieved with the synthesized catalysts at 573 K. Both the synthesized β -MoO₃/Fe₂O₃ catalysts and the reference α -MoO₃ sample had relatively low CO₂ selectivities (3-6%), whereas the support α -Fe₂O₃ with a CO₂ selectivity of about 80% was much less selective for methanol oxidation to formaldehyde. An increase in CO₂ selectivity was found for further decreasing Mo loadings to 0.5%, which can be due to the low β -MoO₃ loading resulting in a sub-monolayer coverage (**Figure S5** and Table S2).^[28] For β -MoO₃/Fe₂O₃ catalysts calcined at different temperatures, a small increase in CO₂ selectivity was found when increasing the calcination temperature (Figure 6B and Figure S5).

In addition, the formation of CO, dimethyl ether, methyl formate, and DMM was also analyzed (Figure S6 and corresponding discussion) indicating that the selective oxidation of methanol over the catalyst MoFe5-673 mainly led to the desired product formaldehyde, about 4% of CO₂, and a very small amount of dimethyl ether and methyl formate, and that no CO and DMM were monitored under the experimental conditions applied.

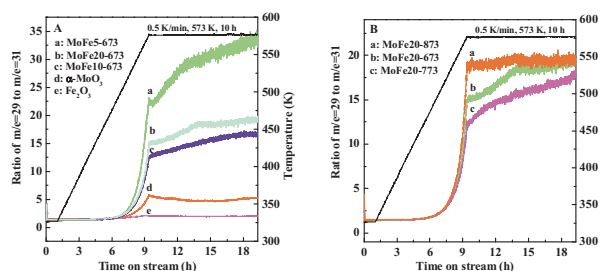


Figure 7. Ratio of $m/e = 29 : m/e = 31$ for the catalysts synthesized with different (A) Mo loadings and (B) calcination temperatures.

Due to the difficult formaldehyde calibration, the ratio of the ion currents of $m/e = 29$ to $m/e = 31$ was used to monitor the formaldehyde formation during the catalytic reaction. As shown in **Figure 7A**, α -Fe₂O₃ hardly achieved any formaldehyde formation, and the production of formaldehyde over bulk α -MoO₃ was much lower than over the synthesized β -MoO₃/Fe₂O₃ catalysts. The catalysts with the lowest Mo loading (MoFe5-673) exhibited the

highest yield of formaldehyde. Additional experiments indicate that the maximum formaldehyde production occurred over the β - $\text{MoO}_3/\text{Fe}_2\text{O}_3$ catalyst with 1% nominal Mo loading (Figure S7). For the β - $\text{MoO}_3/\text{Fe}_2\text{O}_3$ catalysts with calcination temperatures in the range from 673 K to 873 K, there was little influence on the formaldehyde production (Figure 7B), and the catalyst MoFe20-873-24h displayed the highest formaldehyde production rate (Figure S7).

In summary, β - MoO_3/α - Fe_2O_3 catalysts were synthesized for the first time by the one-step CVD of $\text{Mo}(\text{CO})_6$ on α - Fe_2O_3 particles in the presence of O_2 . The synthesized samples with Mo loadings of 5 - 20% exhibited a uniform shell-core structure consisting of homogenous β - MoO_3 thin films with a thickness of 2 - 8 nm supported on the α - Fe_2O_3 particle cores. The structure of the metastable β - MoO_3 film was well retained even after calcination in air at 873 K due to strong Mo-O-Fe links at the interface. The shell-core β - $\text{MoO}_3/\text{Fe}_2\text{O}_3$ catalysts had a much higher catalytic activity and a comparable selectivity than the reference α - MoO_3 catalyst in the selective oxidation of methanol to formaldehyde.

Experimental Section

β - MoO_3/α - Fe_2O_3 catalysts were synthesized using a one-step CVD method followed by calcinations in air. α - Fe_2O_3 (Alfa, 99%) and $\text{Mo}(\text{CO})_6$ (ABCR, 98%) were used as the substrate and the molybdenum precursor, respectively. The CVD set-up was installed in a drying oven, where the sublimation temperature was controlled by the oven. A vertical quartz reactor (i. d. 20 mm) and a glass sublimator (100 ml) were connected by a glass tee, and an oxidizing gas and a carrier gas were introduced into the reactor by the tee and the sublimator, respectively. A vacuum pump was connected to the set-up to enable the synthesis to proceed at desired lowered pressure. The substrate temperature was controlled by an additional resistance heating band, which was fixed around the reactor together with a thermocouple. In a typical synthesis, 2.0 g of Fe_2O_3 were placed in the reactor and a predetermined amount of $\text{Mo}(\text{CO})_6$ in the sublimator. The substrate Fe_2O_3 was dehydrated at 393 K for 2 h in a He flow of 100 Nml/min. Then, the substrate temperature was increased to 473 K in the same atmosphere using a constant heating rate of 10 K/min. Simultaneously, the pressure was decreased to 180 - 200 mbar step by step, and the sublimator temperature was increased to 353 K. The deposition of $\text{Mo}(\text{CO})_6$ was carried out at 473 K by simultaneously introducing 50 sccm of He as carrier gas from the sublimator operated at 353 K and 50 sccm of synthetic air as oxidizing gas from the tee for 2 h. After the deposition, the pressure was increased to atmospheric pressure, and then the reactor temperature was increased to 673 K at a ramp of 10 K/min and the temperature was kept for 2 h in the same atmosphere.

Received: ((will be filled in by the editorial staff))

Published online on ((will be filled in by the editorial staff))

Keywords: β - MoO_3 film · shell-core catalyst · chemical vapour deposition · selective methanol oxidation

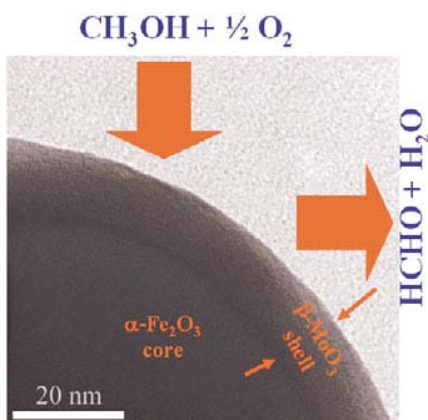
- [1] P. Serp, P. Kalck, R. Feurer, *Chem. Rev.* **2002**, *102*, 3085-3128.
- [2] A. K. Kakkur, *Chem. Rev.* **2002**, *102*, 3579-3588.
- [3] a) R. Schlögl, S. B. Abd Hamid, *Angew. Chem. Int. Ed.* **2004**, *43*, 1628-1637; b) R. Schlögl, *Angew. Chem. Int. Ed.* **2011**, *50*, 6424-6426; W. Zhang, A. Trunschke, R. Schlögl, D. S. Su, *Angew. Chem. Int. Ed.* **2010**, *49*, 6084-6089.
- [4] A. T. Bell, *Science* **2003**, *299*, 1688-1691.
- [5] M. A. B. de Moraes, B. C. Trasferetti, F. P. Rouxinol, R. Landers, S. F. Durrant, J. Scarminio, A. Urbano, *Chem. Mater.* **2004**, *16*, 513-520.
- [6] S. Barazzouk, R. P. Tandon, S. Hotchandani, *Sens. Actuators B* **2006**, *119*, 691-694.
- [7] J. Haber, E. Lalik, *Catal. Today* **1997**, *33*, 119-137.
- [8] L. Zheng, Y. Xu, D. Jin, Y. Xie, *Chem. Mater.* **2009**, *21*, 5681-5690.
- [9] M. Ferroni, V. Guidi, G. Martinelli, P. Nelli, M. Sacerdoti, G. Sberveglieri, *Thin Solid Films* **1997**, *307*, 148-151.
- [10] J. Zou, G. L. Schrader, *J. Catal.* **1996**, *161*, 667-686.
- [11] T. Tsunoda, T. Hayakawa, Y. Imai, T. Kameyama, K. Takehira, K. Fukuda, *Catal. Today* **1995**, *25*, 371-376.
- [12] L. E. Firment, A. Ferretti, *Surf. Sci.* **1983**, *129*, 155-176.
- [13] a) K. Routray, W. Zhou, C. J. Kiely, W. Grünert, I. E. Wachs, *J. Catal.* **2010**, *275*, 84-98; b) S. V. Merzlikin, N. N. Tolkachev, L. E. Briand, T. Strunskus, C. Wöll, I. E. Wachs, W. Grünert, *Angew. Chem. Int. Ed.* **2010**, *49*, 8037-8041; c) K. Routray, W. Zhou, C. J. Kiely, I. E. Wachs, *ACS Catal.* **2011**, *1*, 54-66.
- [14] a) S. C. Street, D. W. Goodman, *J. Vac. Sci. Technol. A* **1997**, *15*, 1717-23; b) X. Xu, W. S. Oh, D. W. Goodman, *Langmuir* **1996**, *12*, 4877-4881.
- [15] J. S. Chung, R. Miranda, C. O. Bennett, *J. Catal.* **1988**, *114*, 398.
- [16] C. J. Machiels, A. W. Sleight, in *Proc. 4th Intern. Conf. on the Chemical Uses of Molybdenum* (Eds: H. F. Barry, P. C. H. Mitchell), **1982**, p. 411.
- [17] W. E. Farneth, F. Ohuchi, R. H. Staley, U. Chowdhry, A. W. Sleight, *J. Phys. Chem.* **1985**, *89*, 2493-2497.
- [18] J. N. Yao, K. Hashimoto, A. Fujishima, *Nature*, **1992**, *355*, 624-626.
- [19] P. A. Spevack, N. S. McIntyre, *J. Phys. Chem.* **1993**, *97*, 11020-11030.
- [20] C. H. F. Peden, G. S. Herman, I. Z. Ismagilov, B. D. Kay, M. A. Henderson, Y. Kim, S. A. Chambers, *Catal. Today* **1999**, *51*, 513-519.
- [21] a) A. Abdellaoui, G. Leveque, A. Donnadieu, A. Bath, B. Bouchikhi, *Thin Solid Films*, **1997**, *304*, 39-44; b) E. Lamouroux, M. Corrias, L. Ressler, Y. Kihn, P. Serp, P. Kalck, *Chem. Vap. Deposition* **2008**, *14*, 275-278.
- [22] E. M. McCarron III, *Chem. Commun.* **1986**, 336-338.
- [23] A. P. S. Dias, V. V. Rozanov, J. C. B. Waerenborgh, M. F. Portela, *Appl. Catal. A* **2008**, *345*, 185-194.
- [24] J. Y. Zou, G. L. Schrader, *Thin Solid Film* **1998**, *324*, 52-62.
- [25] S. S. Al-Shihry, S. A. Halawy, *J. Mol. Catal. A* **1996**, *113*, 479-487.
- [26] A. A. Belhekar, S. Ayyappan, A. V. Ramaswamy, *J. Chem. Tech. Biotechnol.* **1994**, *59*, 395-402.
- [27] A. P. V. Soares, M. F. Portela, *Catal. Rev.* **2004**, *47*, 125-174.
- [28] H. Yamada, M. Niwa, Y. Murakami, *Appl. Catal. A* **1993**, *96*, 113-123.

Entry for the Table of Contents

Methanol oxidation

Guojun Shi, Thomas Franzke, Miguel D. Sánchez, Wei Xia, Frederik Weis, Martin Seipenbusch, Gerhard Kasper, Martin Muhler*, _____ **Page – Page**

Thin-film β - MoO_3 Supported on α - Fe_2O_3 as Shell-Core Catalyst for the Selective Oxidation of Methanol to Formaldehyde



Methanol oxidation: β - MoO_3/α - Fe_2O_3 catalysts synthesized by CVD exhibit a uniform shell-core structure. The structure of the metastable β - MoO_3 film was well retained even after calcination in air at 873 K due to strong Mo-O-Fe links at the interface. The shell-core β - MoO_3/α - Fe_2O_3 catalysts had a much higher catalytic activity and a comparable selectivity than the reference α - MoO_3 catalyst in the selective oxidation of methanol to formaldehyde.

Supporting information

Thin-film β - MoO_3 Supported on α - Fe_2O_3 as Shell-Core Catalysts for the Selective Oxidation of Methanol to Formaldehyde

*Guojun Shi, Thomas Franzke, Miguel D. Sánchez, Wei Xia, Frederik Weis, Martin Seipenbusch, Gerhard Kasper, Martin Muhler**

Steady state tests were performed in a fixed-bed U-tube reactor with an inner diameter of 4 mm (glass lined tube, SGE). The stainless steel U-tube reactor was coated with glass in the inner surface to decrease the wall effect. About 0.15 g of catalyst (sieve fraction 250-355 μm) were sandwiched by quartz wool in the reactor. The catalyst was first pretreated at 673 K at 100 sccm of 10% O_2/He for 1 h. After cooling to 323 K in the same atmosphere, the sample was purged by pure He, and then exposed to 50 sccm of 3000 ppm methanol in He and 50 sccm of 3000 ppm O_2 in He. The composition of the effluents was recorded by an online quadrupole mass spectrometer (QMS, GAM445, BALZERS), which was calibrated with corresponding standard gases.

The BET surface area, pore volume and pore size distribution were determined by static nitrogen physisorption at 77 K (Quantachrome Autosorb-1-MP) after outgassing at 573 K.

Measurements of atomic emission spectroscopy with inductively coupled plasma (ICP-OES) were performed using a UNICAM PU 7000.

Powder XRD tests were carried out in a Philips X'Pert MPD system with a Cu K_α radiation.

Fourier transform infrared (FTIR) spectroscopy was measured in a Vector 22 FTIR spectrometer (resolution: 4 cm^{-1} , 52 scans per measurement). The self-supporting wafer was prepared using the KBr pressing technique with 300 mg of KBr mixed with 1.5 mg of catalysts.

Transmission electron microscopy (TEM) analysis was carried out using a Philips CM12 transmission microscope (120 kV). The samples were prepared by dipping a carbon-coated Cu grid on the dry powder samples.

Scanning electron microscopy (SEM) was performed in a high-resolution thermally aided field spectrometer (Zeiss, LEO 1530 Gemini).

XPS measurements were performed in an ultra-high vacuum set-up equipped with a Gamdata-Scienta SES 2002 analyzer.

Monochromatic Al K_α (1486.6 eV; 14.5 kV, 45 mA) was used as incident radiation. The spectra were taken at 200 eV pass energy (high pass energy mode) at a base pressure better than 3×10^{-10} mbar. The obtained binding energies were determined with an overall resolution better than 0.2 eV. Charging effects were compensated by a flood gun. The C 1s binding energy from adventitious hydrocarbon was applied as a charge reference and fixed at 284.8 eV. The spectrum deconvolution was achieved using the CasaXPS software with Shirley-type background subtraction and with sums of asymmetric Gaussian-Lorentzian functions. The atomic ratios were estimated based on the peak areas, which were corrected with the corresponding atomic sensitivity factors after background subtraction.

NH_3 TPD tests were performed in a quartz U-tube reactor (i.d. 7 mm). About 100 mg of pelletized sample (sieve fraction 250-355 μm) was loaded in the reactor. The catalyst was pretreated in a He flow of 100 sccm at 673 K for 1 h and then cooled to 373 K. 4000 ppm of NH_3 in He was introduced into the catalyst bed to saturate the catalyst for 2 h at 373 K followed by purging with 100 sccm of He for 2 h to remove physically adsorbed NH_3 . Then, the reactor temperature was decreased to 323 K in the same atmosphere. The NH_3 TPD experiment was performed under a helium flow of 100 sccm with a temperature ramp of 5 K min^{-1} from 323 to 923 K. NH_3 TPD patterns were recorded by using a non-dispersive IR detector (BINOS, ROSEMOUNT EMERSON).

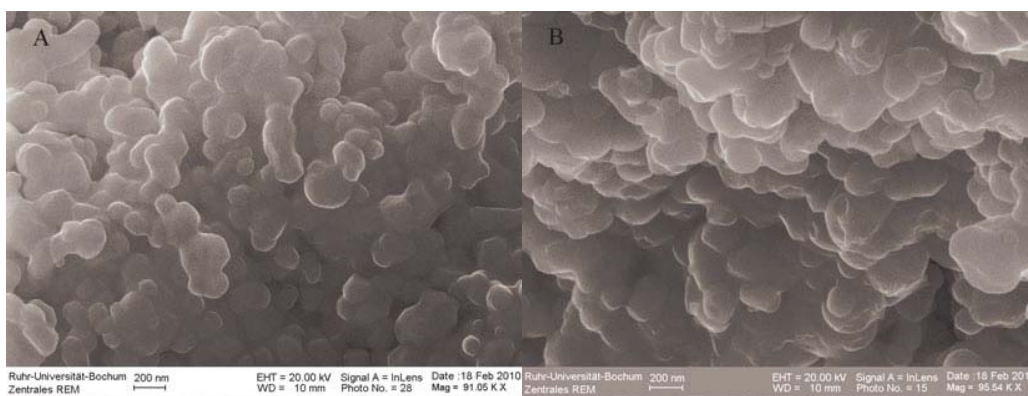


Figure S1 SEM images of (A) Fe_2O_3 and (B) MF20-400.

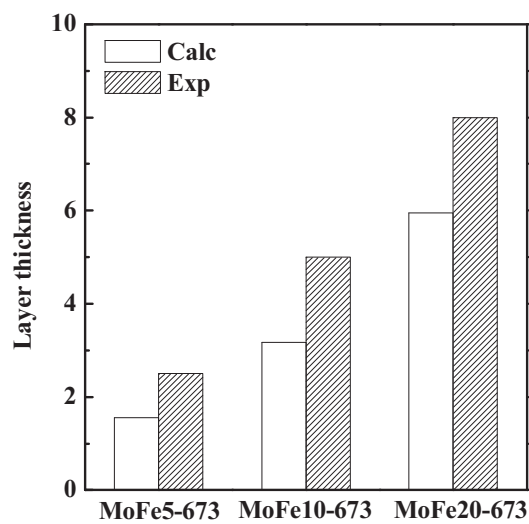


Figure S2. The comparison of $\beta\text{-MoO}_3$ film thicknesses derived from TEM with the calculated ones.

Table S1. Mo 3d binding energies and surface element concentrations

Sample	Binding energy (eV)		Mo concentration (atom. %)			Mo/Fe	FWHM (Mo(VI)) (eV)
	Mo(V)	Mo(VI)	Mo	Mo(V)/Mo	Mo(VI)/Mo		
MoFe5-673	231.7	232.8	20.1	7.2	92.8	9.6	1.12
MoFe10-673	231.9	232.9	21.5	9.9	90.1	19.5	1.06
MoFe20-673	232.8	231.8	19.3	8.8	91.2	19.5	1.02

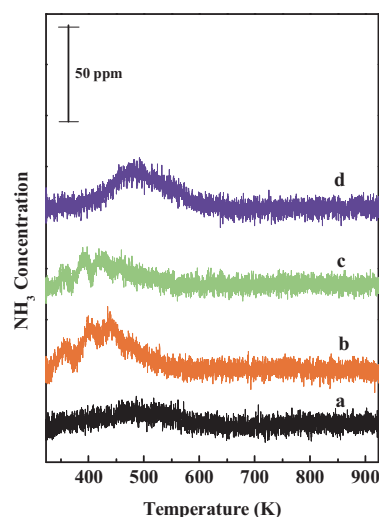


Figure S3. NH₃-TPD patterns of (a) Fe₂O₃, (b) MoFe5-673, (c) MoFe10-673 and (d) MoFe20-673.

The surface acidity of the synthesized catalysts and the substrate α -Fe₂O₃ were probed by NH₃ TPD experiments. As seen from Figure S3, all samples expose a relatively low amount of acidic sites, which should partially be due to the low specific surface area. α -Fe₂O₃ showed very weak surface acidity. The surface acidic sites changed significantly due to the loading of MoO₃. A change in the surface acidity was found according to the NH₃ TPD patterns when decreasing the thickness of the β -MoO₃ film below monolayer coverage resulting in an increasing effect of the α -Fe₂O₃ core and the Mo-O-Fe linking species (Figure S3).

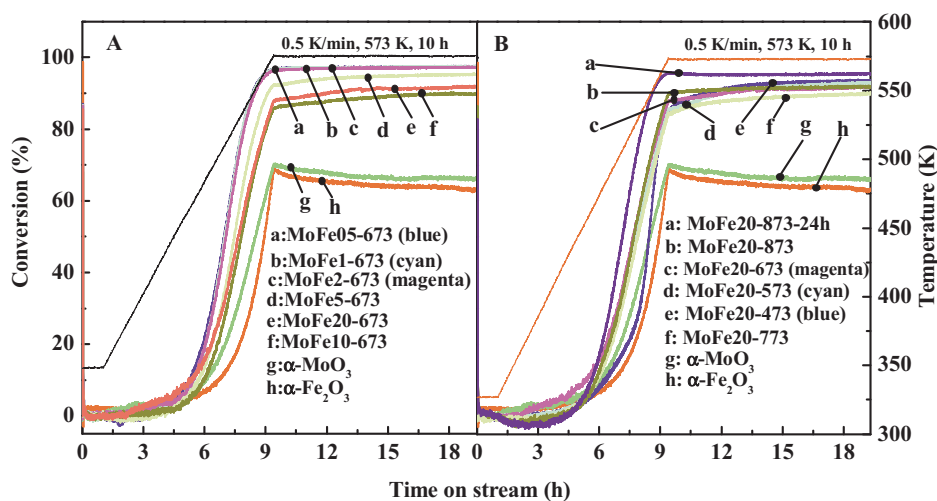


Figure S4. Methanol conversion on the catalysts prepared with different (A) Mo loadings and (B) calcination temperatures. MF20-600-24h was post-treated in flowing air for 24 h.

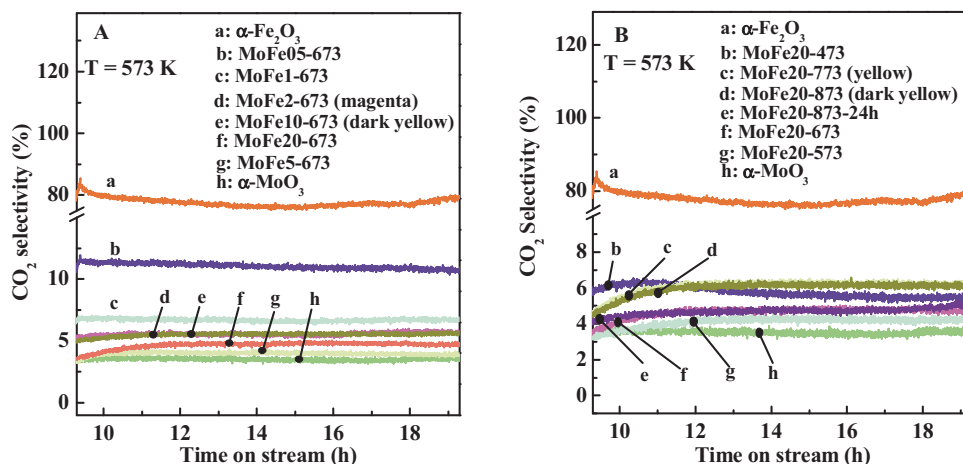


Figure S5. CO₂ selectivities of the catalysts synthesized with different (A) Mo loadings and (B) calcination temperatures.

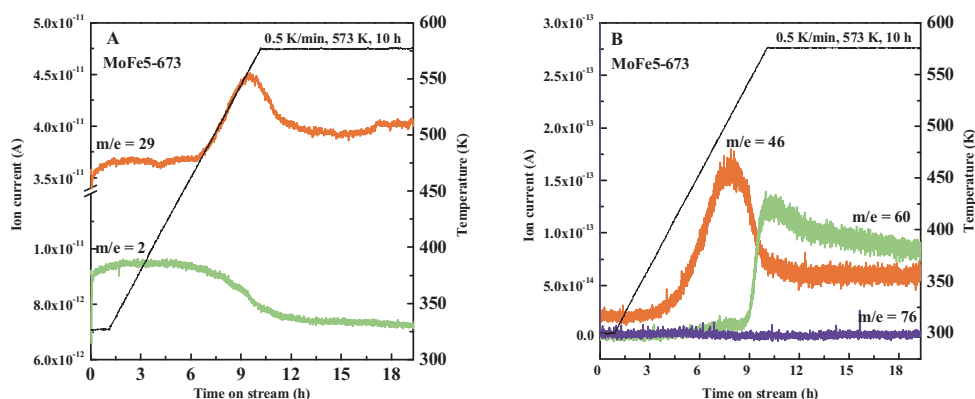


Figure S6. Dependence of ion currents on time on stream over the MoFe5-673 catalyst: (A) m/e = 2 and 29, and (B) m/e = 46, 60 and 76.

The dependence of the ion currents of the possible byproducts except CO₂ on the reaction temperature are shown in Figure S6. H₂ was monitored at m/e = 2, formaldehyde at m/e = 29, dimethyl ether at m/e = 46, methyl formate at m/e = 60 and dimethoxymethane at m/e = 76. The ion current at m/e = 29 increased with increasing reaction temperature from 323 K to 573 K, then it leveled off after 2 h of time on stream at this temperature. The ion current at m/e = 2 was 2 orders of magnitude lower than that at m/e = 29, and its intensity at m/e = 2 decreased with increasing reaction temperature, indicating that H₂ production in the reaction was negligible. The ion current at m/e = 2 was due to the contribution of methanol, which decreased with increasing temperature because of the increasing methanol conversion. In the presence of water, the absence of H₂ confirmed that there was no CO production in the reaction according to the water gas shift equilibrium (WGS, equation (S1)) in the presence of α-Fe₂O₃.



The ion currents at m/e = 46 and 60 showed an increase with increasing reaction temperature. However, the absolute value of the ion currents were 2-3 orders of magnitude lower than the ion current at m/e = 29, indicating that there was a very small amount of dimethyl ether and methyl formate produced in the reaction. The ion current at m/e = 76 showed no dimethoxymethane being formed in the reaction. According to the analysis of the possible byproducts in the reaction, it is safe to say that selective oxidation of methanol over the catalyst MoFe5-673 mainly led to the desired formaldehyde, about 4% of CO₂, and a very small amount of dimethyl ether and methyl formate, and that no CO and dimethoxymethane were monitored under the experimental conditions applied.

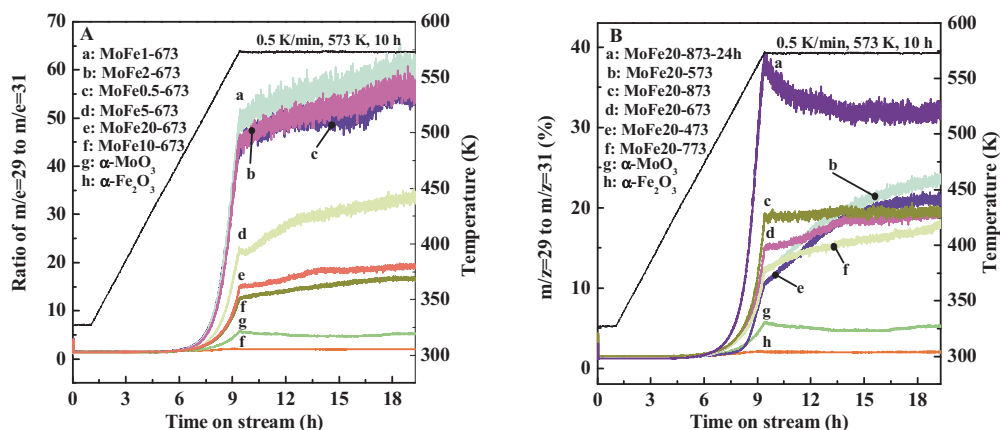


Figure S7. Ratio of $m/e = 29 : m/e = 31$ on the catalysts prepared with different (A) Mo loadings and (B) calcination temperatures.

Table S2. The surface concentration of Mo atom on the catalysts synthesized with different loadings

Sample	MoFe05-673 ^[a]	MoFe1-673 ^[a]	MoFe2-673 ^[a]	MoFe5-673	MoFe10-673	MoFe20-673
S_{BET} (m^2/g)	6.2	6.2	6.2	7.4	6.4	6
Mo loading (wt%)	0.59	1.2	2.3	4.7	9.1	15.8
Surf. conc. (nm^{-2})	6.0	11.9	23.5	39.8	89.2	165.1

[a] Calculated according to the nominal loadings and the specific surface area of the substrate $\alpha\text{-Fe}_2\text{O}_3$.